BIOINFORMATICS ORIGINAL PAPER

Vol. 28 no. 20 2012, pages 2608–2614
doi:10.1093/bioinformatics/bts493

Structural bioinformatics

Application of asymmetric statistical potentials to antibody–protein docking

Ryan Brenke[1,**], David R. Hall[1,**], Gwo-Yu Chuang[1,**], Stephen R. Comeau[1], Tanggis Bohnuud[1], Dmitri Beglov[1], Ora Schueler-Furman[2], Sandor Vajda[1,*] and Dima Kozakov[1,*]

[1]Department of Biomedical Engineering, Boston University, Boston, MA, USA, and [2]Department of Microbiology and Molecular Genetics, The Hebrew University, Jerusalem, Israel

Associate Editor: Anna Tramontano

ABSTRACT

Motivation: An effective docking algorithm for antibody–protein antigen complex prediction is an important first step toward design of biologics and vaccines. We have recently developed a new class of knowledge-based interaction potentials called Decoys as the Reference State (DARS) and incorporated DARS into the docking program PIPER based on the fast Fourier transform correlation approach. Although PIPER was the best performer in the latest rounds of the CAPRI protein docking experiment, it is much less accurate for docking antibody–protein antigen pairs than other types of complexes, in spite of incorporating sequence-based information on the location of the paratope. Analysis of antibody–protein antigen complexes has revealed an inherent asymmetry within these interfaces. Specifically, phenylalanine, tryptophan and tyrosine residues highly populate the paratope of the antibody but not the epitope of the antigen.

Results: Since this asymmetry cannot be adequately modeled using a symmetric pairwise potential, we have removed the usual assumption of symmetry. Interaction statistics were extracted from antibody–protein complexes under the assumption that a particular atom on the antibody is different from the same atom on the antigen protein. The use of the new potential significantly improves the performance of docking for antibody–protein antigen complexes, even without any sequence information on the location of the paratope. We note that the asymmetric potential captures the effects of the multi-body interactions inherent to the complex environment in the antibody–protein antigen interface.

Availability: The method is implemented in the ClusPro protein docking server, available at http://cluspro.bu.edu.

Contact: midas@bu.edu or vajda@bu.edu

Supplementary information: Supplementary data are available at *Bioinformatics* online.

Received on November 20, 2011; revised on July 27, 2012; accepted on August 2, 2012

1 INTRODUCTION

Protein–protein docking methods have significantly improved in the last few years. According to the last round of the blind protein docking experiment CAPRI (Lensink and Wodak, 2010), automated protein docking servers performed comparably well with the top human predictor groups, without the use of biological information. In particular, our protein docking server ClusPro was the top protein docking server, as well as within the top 10 of all predictors. Despite these improvements, the docking of an antibody to its protein antigen, an important first step toward computational design of biologics and vaccines, remains particularly challenging for both ClusPro and other methods (Ponomarenko and Bourne, 2007; Vajda, 2005). We note that although we focus on interactions between antibodies and proteins, for simplicity we define the problem as antibody–antigen docking. It is no doubt that the relatively weak performance represents the state of art in protein docking. In fact, Ponomarenko and Bourne (2007) found ClusPro to better predict epitopes than methods that have been specifically developed for such predictions, although they used an earlier and less accurate version of the server. It is easy to see why docking antigen–antibody pairs is much more difficult than docking inhibitors to enzymes. Enzyme–inhibitor complexes generally exhibit excellent surface complementarity, with the convex inhibitor matching the concave binding site of the enzyme (Vajda, 2005). Most of the native enzyme–inhibitor interfaces also have favorable hydrophobic and polar interactions, which facilitate docking and scoring (Vajda, 2005). In contrast, the interfaces in antibody–antigen complexes are mostly flat and less hydrophobic (Lo Conte et al., 1999). The flat interface implies that searching for surface complementarity provides little help in docking. In addition, the polar interactions are more sensitive to atomic positions than the hydrophobic ones, and hence scoring based on molecular mechanics energy functions including electrostatics becomes less reliable due to the inevitable conformational differences between free and bound protein structures. Thus, it is very important to develop scoring functions that account for these specific properties of the interface and can help finding near-native complex structures.

It was shown by several groups that the inclusion of structure-based potentials in the energy function used for the docking can significantly improve performance (Chen *et al.*, 2003; Kozakov *et al.*, 2006; Ravikant and Elber, 2010). Here, we describe the development and testing of an accurate pairwise interaction potential specific to antibody–antigen complexes. Based on statistical mechanics, structure-based potentials are traditionally derived from the 'inverse Boltzmann' principle (Sippl, 1993), assuming that frequently observed structural states are low energy states. In the first-order approximation,

*To whom correspondence should be addressed.
**The authors wish it to be known that, in their opinion, the first three authors should be regarded as joint First Authors.

molecular interactions can be decomposed as the sum of pairwise atom–atom interactions. The energy of interaction can be written as:

$$\varepsilon_{IJ} = -kT\ln\left(\frac{p_{IJ}^{\text{obs}}}{p_{IJ}^{\text{ref}}}\right),$$

where k is the Boltzmann constant, T the temperature, p_{IJ}^{obs} the probability of interactions between atoms of types I and J in an observed set (e.g. crystal structures) and p_{IJ}^{ref} is the probability of atoms of types I and J being within the interaction distance, in a state without any atom-type-specific interactions, the 'reference state'. We have recently reported a pairwise interaction potential called Decoys as the Reference State (DARS) (Chuang *et al.*, 2008). The idea of DARS is generating a large set of docked conformations with good shape complementarity but without accounting for atom types, and using the frequency of interactions extracted from these DARS. In principle, the resulting potential is ideal for finding near-native conformations among structures obtained by docking and can be combined with other energy terms to be used directly in docking calculations. Accordingly, we incorporated DARS into the energy function used by our docking program PIPER (Kozakov *et al.*, 2006). Based on the fast Fourier transform (FFT) correlation approach, PIPER can perform global docking of unbound protein structures without any *a priori* information on the structure of the complex and was the best performing method in the latest round of the CAPRI protein docking experiment (Lensink and Wodak, 2010). DARS improved the docking results for all classes of complexes. For enzyme–inhibitor pairs, DARS provides both excellent discrimination and docking results, even with very small decoy sets. With a few exceptions, the DARS docking results are also good for complexes that occur in signal transduction pathways. However, for antibody–antigen pairs, results were substantially worse than for other types of complexes, although DARS performed slightly better than some earlier interaction potentials. The results were poor even when the location of the complementarity determining regions (CDRs) on the antibody was determined based on sequence information and the search was constrained to include the CDRs in the interface.

Analyzing the potential sources of poor performance for antibody–antigen pairs, we arrived at the conclusions that the main problem is the inherent asymmetry of the interface in these types of complexes (Chuang *et al.*, 2008). We recall that the pairwise structure-based potentials to model protein–protein interactions automatically assume the symmetry of interactions between atoms on the two sides of the interface, i.e. that

$$\varepsilon_{I_{\text{rec}}J_{\text{lig}}} = \varepsilon_{J_{\text{rec}}I_{\text{lig}}},$$

where I_{rec}, J_{rec} are atom types on the receptor and I_{lig}, J_{lig} are atom types on the ligand. However, it is easy to show that the assumption of symmetry limits the performance of the potential in antibody–antigen docking. As shown in Figure 1, there is usually a large, hydrophobic region on the paratope of the antibody, containing a large number of tyrosines, tryptophans and phenylalanines, thus these three residues occur with high frequency in the interface. This is supported by residue interaction statistics gathered on the antibody–protein interaction dataset, as shown in Supplementary Table S1. Based on these statistics,

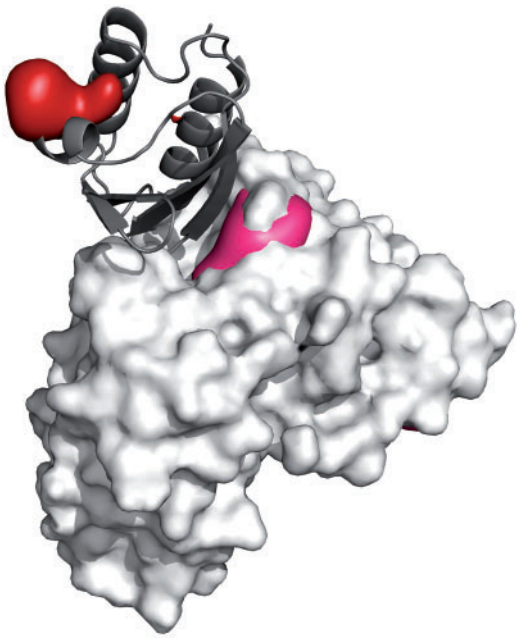

Fig. 1. Patches of maximum hydrophobicity in an antibody–antigen complex. The structure is Jel42 Fab fragment complexed with HPr (PDB code 2jel). The antibody fragment is shown as the white solid model, with magenta patches representing the regions with maximum hydrophobicity. The HPr antigen is shown as a gray cartoon, with dark red patches as regions of maximum hydrophobicity. In the figure, the antibody CDR is oriented upward, showing that the CDR region includes strongly hydrophobic patches, but these do not interact with regions of maximum hydrophobicity on the HPr antigen

interactions between the atoms of these residues and any other atom on the other side of the interface appear to be favorable, resulting in a large negative pairwise energy term. Addition of this term will improve the location of the interface and thus the near-native conformation if these residues are on the paratope of the antibody. However, the tyrosines, tryptophans and phenylalanines on the antigen side are not found in the epitope with any higher frequency than on any other part of the protein. Thus, a favorable interaction term for these residues on the antigen leads to false positives, incorrectly predicting that any region of the antigen rich in these residues is likely to be part of the epitope, which is generally not the case.

The concept of symmetry is generally accepted for pairwise potentials because interaction forces between two isolated atoms or molecules are symmetric. Most structure-based potentials have been derived from folded protein structures (Lu and Skolnick, 2001; Miyazawa and Jernigan, 1985; Rojnuckarin and Subramaniam, 1999; Skolnick *et al.*, 1997) where the symmetric pairwise assumption, ignoring multi-body interaction terms, was the natural first choice. These potentials proved to be successful for folding and, later on, for docking, so the assumption of symmetry has not been questioned. As discussed, antibody–antigen interactions clearly do not fit this framework. Although the deviation from symmetry may be surprising, it is important to note that interactions between atoms are not pairwise, and the latter assumption is just a convenient approximation. Thus, the

pairwise energy terms, extracted from the frequency of specific interactions observed in protein structures or complexes, represent an empirical measure of interaction strength rather than real physical forces. Developing multi-body interaction potentials would be a more rigorous approach than restricting consideration to pairwise interaction, but we have far from enough data for the parameterization of such potentials.

Here, we suggest an alternative approach, simply removing the requirement of interaction symmetry. The resulting potential preserves the general form and computational simplicity of statistical potentials, but to a certain degree accounts for the local environment of an atom and thus introduces some elements of multi-body potentials. To our knowledge, no asymmetric potentials have been previously reported for predicting protein–protein interactions. We describe the development of the asymmetric DARS-type potential, called ADARS, based on a non-redundant dataset of antibody–antigen complexes extracted from the Protein Data Bank (PDB). ADARS has been integrated into the energy function used in the docking program PIPER, and tested on an antibody–antigen docking benchmark. We demonstrate significant improvements in the docking results, when compared with earlier symmetric potentials. The resulting antibody–antigen docking protocol is included in our ClusPro protein docking server, which is freely available.

2 METHODS

2.1 Potential development

2.1.1 Selection of non-redundant antibody–antigen dataset A DARS potential requires defining the native training set and the reference set from which to extract the atom-type contacts. For training our original DARS potential, we used the non-redundant database of native protein–protein complexes from Glaser *et al.* (2001). This set includes 621 protein interfaces from 492 PDB entries. As previously noted (Chuang *et al.*, 2008), the set was biased toward homodimers and enzyme–inhibitor complexes that tend to have excellent pairing of hydrophobic regions on the two sides of the interface, which is not the case in antibody–antigen interactions.

For the antibody–antigen-specific DARS, we have extracted all the records containing antibodies from the PDB that were solved by either X-ray crystallography (with resolution up to 4 Å) or nuclear magnetic resonance. After removing unbound antibody structures, we ended up with 199 antibody–protein complexes. We assign the antibody chains as the receptor. We clustered all the ligands with over 30% sequence identity. The resulting clusters were manually inspected for redundancy in terms of different binding modes [>9 Å ligand root mean square deviation (RMSD)] or different antibody sequence (>30% sequence difference at the interface). We have also retained some antibody–antibody complexes, such as anti-idiotype complexes, which mimic antibody–antigen complexes. We then removed from our training set all complexes in the protein–protein docking benchmark (Hwang *et al.*, 2008) set and the ones similar to them, based on redundancy criteria described above. What remained was a set of 99 non-redundant complexes, a training set appropriate for our purpose. All heteroatoms and water molecules were removed prior to analysis. The final list of complexes is provided as Supplementary Material (Table S2).

2.1.2 Atom-type selection Such a small training set provides limited statistics of interactions between atoms on the two sides of the interface. In order to avoid an underdetermined statistical problem when estimating the atom pair interactions energies, we reduced the number of atom types. As already mentioned, hydrophobicity is major driving force in antibody/antigen interactions, and tyrosine, tryptophan and phenylalanine occur with high frequency in the paratope (Halperin *et al.*, 2002); hence, from the 18 atom types of DARS, we selected FC^{ζ}, YC^{ζ} and LC^{δ} that represent the atom types mainly involved in these interactions. As defined by Zhang *et al.* (1997), FC^{ζ} includes all the ring carbon atoms in Phe and Trp, as well as the three proximal phenolic ring atoms in Tyr (C^{γ}, $C^{\delta 1}$ and $C^{\delta 2}$). YC^{ζ} denotes the three distal phenolic ring atoms in Tyr that appear to be influenced by the terminal hydroxyl group and thus need to be treated separately. The terminal carbon atoms in Ile, Leu, Met and Val constitute the third group, LC^{δ}. All other atoms are placed into a single 'other' atom type. Using just four types ensures that all training data bins will be well populated. The choice of atom types is based on our understanding of antibody–antigen interactions and the statistics of interactions observed in the training set (shown in Supplementary Tables S1 and S3). Although the decision is supported by the results described below—it is by no means optimized. For example, it was observed that there is high frequency of Ser on antibody interfaces (Clark *et al.*, 2006). Thus, adding specific serine atom types would be a natural choice once more antibody–antigen complexes are available for constructing the potential.

2.1.3 Reference set The main feature of DARS is the selection of a set of complexes as the reference set. From each of these, a set of docked structures is generated, using shape complementarity as the docking energy function. For our reference set, we have randomly selected 15 of these 100 antibody–antigen complexes. During docking, only the Fv region of the antibody (antigen-binding fragment of the antibody that includes variable domains of the heavy and light chains) is considered. For each complex, we use the van der Waals energy function of PIPER to generate 5000 shape complementarity decoys. (PIPER is described in more detail below.) We then determined the reference state probability based on the frequencies of atom–atom interactions in the decoy set (Chuang *et al.*, 2008):

$$P_{IJ}^{\mathrm{ref}} = \frac{\nu_{IJ}^{\mathrm{ref}}}{\sum_{I,J} \nu_{IJ}^{\mathrm{ref}}},$$

where ν_{IJ}^{ref} is the number of contacts between atoms of types I on the receptor and J on the ligand in the decoy ensemble. The other properties of the antibody–antigen-specific DARS, the contact cutoff distance and the atom-type definitions, were chosen identically to the original DARS. For the contact cutoff distance, atom i of the receptor (the antibody) is considered to interact with atom j of the ligand (the antigen) if their distance r_{ij} is <6 Å.

2.1.4 Description of the potentials compared To better illustrate the effect of introducing asymmetry to pairwise potential, and the role of antibody–antigen-specific training data, we have compared three potentials in this article. The first is the previously developed general DARS (Chuang *et al.*, 2008). The second potential, symmetric antibody–antigen DARS (aDARS), uses four atom types (YC^{ζ}, FC^{ζ}, LC^{δ} and 'other') and is trained on the antibody–antigen training set, but retains the symmetry constraint $\varepsilon_{IJ} = \varepsilon_{JI}$. Finally, the symmetry constraint is removed in the antibody–antigen-specific asymmetric DARS (aADARS), and thus we effectively have four antibody atom types (antibody YC^{ζ}, FC^{ζ}, LC^{ζ} and 'other'), interacting with four antigen atom types (antigen YC^{ζ}, FC^{ζ}, LC^{ζ} and 'other').

2.2 Antibody–antigen docking benchmark

To test our antibody–antigen-specific DARS potential, we use the antibody–antigen complexes from protein–protein docking benchmark (Hwang *et al.*, 2008). Some complexes were excluded as follows. The complex 2hmi was removed because the bound complex contains

DNA. The complex 1e4k was removed because it is not an antibody–antigen complex: the 'antigen' is actually an Fc receptor, binding the Fc region of the antibody. Finally, three complexes (1i9r, 1k4c and 2vis) were removed as they are complexes of antigen multimers with multiple antibodies, and thus beyond the scope of pairwise docking considered in this article. The remaining 20 cases were used as our test set. As noted above, we have removed all complexes of this benchmark from our training set to prevent biasing our results.

2.3 Docking

For docking, we used our previously developed protein–protein docking program PIPER (Kozakov *et al.*, 2006). PIPER is an FFT-based docking program that uses a structure-based pairwise potential as one component of its energy function. The total energy is the sum of terms representing shape complementarity, electrostatic and desolvation contributions, the last described by the pairwise potential (Kozakov *et al.*, 2006; Chuang *et al.*, 2008):

$$E = E_{\text{vdw}} + w_3 E_{\text{elec}} + w_4 E_{\text{pair}},$$
$$E_{\text{vdw}} = w_1 E_{\text{rep}} + w_2 E_{\text{attr}},$$
$$E_{\text{elec}} = \sum_{i=1}^{N_r}\sum_{j=1}^{N_l} q_i q_j \Big/ \left(r_{ij}^2 + D^2 \exp\left(\frac{-r_{ij}^2}{4D^2}\right)\right)^{\frac{1}{2}},$$
$$E_{\text{pair}} = \sum_{i=1}^{N_r}\sum_{j=1}^{N_l} \varepsilon_{a(i)a(j)},$$

where N_r and N_l denote the numbers of atoms in the receptor and the ligand, respectively. The E_{vdw} term is a stepwise implementation of the van der Waals energy, with E_{attr} and E_{rep} representing its attractive and repulsive components, respectively. E_{elec} is the Coulombic electrostatic energy and E_{pair} denotes the pairwise potential described above. $\varepsilon_{a(i)a(j)}$ is the potential energy between two atoms of types $I = a(i)$ and $J = a(j)$. That is, $a(x)$ is the atom-type mapping of atom number x. r_{ij} is the distance between atom i and j in the protein. $D = max_i(r_i^{\text{vdw}})$, where r_i^{vdw} is Van der Waals radii of atom i. PIPER (Kozakov *et al.*, 2006) is able to incorporate symmetric pairwise potentials within its energy function. Approximating the interaction matrix by its eigenvectors corresponding to the few dominant eigenvalues results in an energy expression written as the sum of a few correlation functions, which can be solved by repeated FFT calculations. Unfortunately, it is not possible to perform eigenvalue decomposition of the $N \times N$ asymmetric matrix M_{asym}. However, we can create an equivalent symmetric potential of the size $2N \times 2N$ as shown below. In this representation, the first N types correspond to the atoms of the antibody, and the subsequent N to the atoms of the antigen. It is easily seen that the interaction energy from the asymmetric matrix is equivalent to the proposed symmetric form. This makes it possible to use ADARS within PIPER.

$$M_{\text{sym}} = \begin{bmatrix} 0 & M_{\text{asym}} \\ M_{\text{asym}}^T & 0 \end{bmatrix}.$$

The translational space of the receptor and ligand energy functions is sampled at a step size of 1.0 Å and the rotational space is sampled approximately every 5°, resulting in 70 000 rotations of the ligand. To prevent bias of the grid placement, each structure is randomly rotated and translated prior to docking.

For each complex, the best scoring 1000 structures are clustered (Kozakov *et al.*, 2005) to produce a number of predictions. We also tested the potentials in conjunction with the commonly used method of 'masking' the non-CDR (i.e. not CDR) parts of the antibody. This effectively limits the docking results to complexes in which the interface includes the CDRs. The residues to mask were determined by Kabat's definition of the CDR (see http://www.bioinf.org.uk/abs/), with three additional residues in each direction remaining unmasked (Kozakov *et al.*, 2006; Chuang *et al.*, 2008).The weighting coefficients $w_1, w2, w3$ are selected based on calorimetric considerations (Chuang *et al.*, 2008). The w_4 coefficient in the energy expression is optimally selected for the particular potential, and hence is different for DARS, aADARS and aDARS (Chuang *et al.*, 2008).

2.4 Assessment of the results

For result assessment, we consider the model a hit if ligand atoms within 10 Å of the receptor in the crystal are within 10 Å RMSD in the model (to ignore the motion of that part of the ligand which is not participating in the interaction). Although 10 Å RMSD may appear to be very large, one has to keep in mind that the prime aim of the FFT sampling and clustering steps is to determine the region of interest in the conformational space, and the structures in this region can be further refined by methods that account at least for side chain and possibly for some backbone flexibility. In a recent paper describing our results in the CAPRI experiment (Kozakov *et al.*, 2010), we showed that such models can indeed be further refined to obtain structures of high quality.

3 RESULTS AND DISCUSSION

3.1 ADARS potential

The antibody–aADARS potential is shown in Table 1. The strongest signal in this potential is from the antibody YC^{ζ} type (i.e. the distal ring atoms of Tyr), interacting atom types FC^{ζ}, LC^{δ} and other on the antigen. This shows that it is energetically favorable for the YC^{ζ} type to be in the paratope regardless of what is in the epitope. The only interaction of YC^{ζ} atoms that are not very favorable are with another atom of the same type. Also strong is the FC^{ζ}–FC^{ζ} interaction between Tyr rings. The strongest repulsive potentials are coming from the antibody hydrophobic LC^{δ} atoms interacting with almost any of the antigen atoms. Thus, the potential illustrates that the somewhat hydrophobic YC^{ζ} atoms of Tyr and the more hydrophobic FC^{ζ} atoms of Phe, Trp and Tyr have a high probability of being at the antibody interface regardless of the residues at the antigen interface, in good agreement with the high frequency of these residues in the CDR regions.

3.2 Docking results

To demonstrate the effects of the asymmetric potential and antibody–antigen-specific training data, we have compared three potentials. The first is the generic DARS potential, which compares favorably to a number of other potentials (Chuang *et al.*, 2008), and used with PIPER for docking helped us to be the best

Table 1. AaDARS potential

Antibody	antigen			
	YC^{ζ}	FC^{ζ}	LC^{δ}	Other
YC^{ζ}	−0.34	−1.48	−1.45	−1.37
FC^{ζ}	−0.14	−0.72	−0.45	−0.46
LC^{δ}	0.38	0.19	0.51	0.86
Other	0.03	−0.08	0.27	0.22

Table 2. Docking using DARS, aDARS and aADARS potentials

		DARS		DARS*		aDARS		aDARS*		aADARS		aADARS*	
complex	Components[a]	Rank	(rmsd)	Rank	(rmsd)	Rank	(rmsd)	Rank	(rmsd)	Rank	(rmsd)	Rank	(rmsd)
1ahw	u/u	—	—	3	(5.34)	5	(5.92)	2	(5.33)	24	(5.74)	6	(5.52)
1bgx	u/u	—	—	—	—	—	—	—	—	—	—	—	—
1bj1	b/u	4	(4.24)	3	(4.33)	4	(6.28)	1	(6.28)	1	(5.40)	1	(4.96)
1bvk	u/u	—	—	—	—	—	—	—	—	28	(5.42)	21	(5.42)
1dqj	u/u	—	—	3	(9.91)	1	(9.64)	1	(9.64)	10	(9.64)	1	(9.51)
1e6j	u/u	2	(2.21)	1	(4.97)	1	(8.34)	1	(8.01)	1	(7.05)	1	(8.40)
1fsk	b/u	1	(1.98)	1	(2.57)	2	(1.62)	1	(1.62)	1	(1.62)	1	(1.62)
1iqd	b/u	1	(7.15)	2	(8.93)	7	(7.20)	9	(7.20)	1	(5.39)	9	(4.74)
1jps	u/u	—	—	1	(4.57)	5	(5.73)	7	(4.39)	14	(7.71)	6	(5.73)
1kxq	b/u	1	(3.51)	5	(5.39)	2	(3.08)	6	(7.09)	2	(3.87)	2	(7.90)
1mlc	u/u	16	(1.90)	12	(4.36)	20	(8.95)	22	(9.21)	6	(9.23)	20	(8.90)
1nca	b/u	—	—	17	(1.81)	—	—	25	(1.93)	30	(2.11)	5	(2.10)
1nsn	b/u	—	—	—	—	—	—	—	—	13	(6.89)	28	(4.00)
1qfw:hl	b/u	1	(3.32)	2	(4.83)	4	(2.76)	1	(3.10)	2	(8.38)	1	(8.38)
1qfw:im	b/u	—	—	18	(3.12)	9	(2.96)	8	(2.96)	7	(6.73)	4	(5.88)
1vfb	u/u	—	—	6	(8.05)	7	(8.76)	4	(8.72)	3	(5.87)	1	(8.31)
1wej	u/u	—	—	13	(1.56)	2	(4.02)	2	(4.02)	1	(3.55)	1	(2.78)
2fd6	u/u	16	(4.08)	8	(4.30)	—	—	11	(1.95)	5	(2.50)	5	(1.95)
2i25	u/u	—	—	18	(3.02)	—	—	3	(7.18)	8	(5.77)	7	(4.08)
2jel	b/u	—	—	3	(3.44)	5	(4.60)	2	(2.77)	2	(2.77)	2	(2.77)

[a]u/u, unbound–unbound; b/u, bound–unbound.
*Masking of non-CDR of the antibody.

performing predictor group in the latest rounds of CAPRI (Lensink and Wodak, 2010). The second potential is the symmetric DARS, but restricted to the four atoms types discussed, and trained on antibody–antigen data (aDARS). Finally, the third potential, referred to as aADARS, is the asymmetric DARS, with four atom types, and trained on the same antibody–antigen data. To evaluate their performance, each of these three potentials was incorporated as the pairwise component of the energy function used in PIPER for docking (see Section 2) (Kozakov *et al.*, 2006), followed by clustering of the top 1000 results (Kozakov *et al.*, 2005), as implemented in our protein–protein docking server ClusPro (Comeau *et al.*, 2004). The potentials were tested on the antibody–antigen complexes of the protein docking benchmark (Hwang *et al.*, 2008). In addition to complexes, the benchmark also includes an unbound structure for at least one of the component proteins. The unbound/unbound or unbound/bound complexes have been used as provided in the benchmark (Hwang *et al.*, 2008). We note that complexes close to the ones in the benchmark set were removed from the training set, following the rules described in Section 2.

In Table 2, the rank of the first cluster with <10 Å C_α RMSD between the bound and predicted ligand structures is reported along with the RMSD of that cluster representative. The absence of a number indicates that no cluster with <10 Å C_α RMSD is predicted. The first column of Table 2 shows the PDB ID of the bound complex. The second column shows whether the case is bound/unbound or unbound/unbound. The third column (DARS) shows the results of docking using the original DARS potential. The fourth column (DARS*) is the same as the third, but with the non-CDR regions of the antibody masked, making them unavailable for the interface. The fifth column (aDARS) shows the results of docking using the antibody–antigen-specific symmetric DARS potential. The sixth column (ADARS*) is the same as the fifth, but with the non-CDR regions of the antibody masked. Analogously, the seventh column (aADARS) shows the results of docking using the aADARS potential and the eights column (aADARS*) is the same as the seventh, but with the non-CDR of the antibody masked. It is clear from Table 2 that aADARS performs better than the other potentials that all are unable to find near-native structures for a number of complexes, whereas using aADARS or aADARS*, this occurs only once.

All methods fail to generate any near-native structure for the complex 1bgx. In principle, docking in this case should not be more difficult than in many others, as the backbone conformational change between the bound and unbound structures is moderate (1.48 Å interface C_α RMSD). Although there are a few large side-chain clashes, these are not expected to lead to major problems as the energy function in PIPER is 'soft' enough to account for potential overlaps. However, the most significant feature of this case is the large size of the antigen (*Taq* DNA Polymerase). FFT-based methods generally provide better performance when the ligand is the smaller molecule. Due to limitations of the current implementation of PIPER with asymmetric potentials, the antibody is required to be the receptor, which is appropriate in the majority of the benchmark cases as antibodies are relatively large. Since in docking the complex, we translate and rotate a large molecule using a predefined grid,

Table 3. Success rate of DARS, aDARS and aADARS potentials

Rank	DARS (%)	DARS* (%)	aDARS (%)	aDARS* (%)	aADARS (%)	aADARS* (%)
Top 1	20	15	10	25	30	35
Top 10	30	60	65	70	70	80
Top 30	40	85	70	85	95	95
Miss	60	15	30	15	5	5

*Masking of non-CDR of the antibody.

the failure may be attributed to insufficient sampling rather than to problems with the scoring function.

The performance of the methods is summarized in Table 3. To understand these results, note that PIPER retains the 1000 lowest energy conformations from the FFT-based search, clusters the retained structures using the pairwise RMSD as the distance measure and selects a number of the largest clusters for refinement and further analysis. Table 3 shows the success rates for retaining 1, 10 or 30 clusters, ranked based on cluster size. Here, success is defined as having a structure with <10 Å C_α RMSD. Note that retaining the top 10 clusters is aligned to the CAPRI rules that allow 10 models to be submitted for each docking target. The case of retaining 30 clusters is considered, because this is the maximum number of clusters that are feasible to process by more detailed refinement methods (Kozakov *et al.*, 2008). According to the results in Table 3, using the original DARS potential PIPER fails to generate near-native structures in the top 30 clusters for 60% of the complexes in the benchmark, and thus is not suited for antibody–antigen docking. Masking the non-CDR regions of the antibody (see DARS[a]) improves the results by decreasing the number of failures to 15%. A symmetric potential trained on antigen–antibody complex data (i.e. aDARS) improves the results relative to the original DARS, however the number of missed targets stays high, and masking is still required to reduce the number of failures. As the last two columns of Table 3 show, the asymmetric potential trained on antibody–antigen complexes (aADARS[a]) yields substantial improvement. In summary, the new potential is a substantial improvement over the original DARS potential.

Considering the CAPRI success criterion (at least one acceptable model among the 10 best predictions), using the bound structure of the antibody does not substantially change performance. The success rates are 89% and 80% for the bound/unbound and unbound/unbound docking problems, respectively, (in the latter case ignoring the problematic 1bgx case discussed above).

It should be noted that the steps described above do not include high-resolution refinement, due to time constraints. However, such refinement can usually improve the quality of the model, as we have repeatedly shown in the CAPRI experiment (Kozakov *et al.*, 2010). We have recently demonstrated (Kozakov *et al.*, 2008) that an initial global FFT-based search is highly complementary to a subsequent local refinement using Monte Carlo-based approaches, as implemented in Rosetta (Gray *et al.*, 2003; Sircar and Gray, 2010).

4 CONCLUSION

Antibody–antigen complexes present a challenge for protein–protein docking due to their less favorable desolvation free energies and more planar interfaces when compared with enzyme–inhibitor complexes. The less favorable desolvation free energies are due in part to their less hydrophobic interfaces. Interestingly, there are a number of hydrophobic atoms in the interface, but mostly on the antibody side, whereas the epitope on the antigen may be less hydrophobic. In fact, this should be the case, as antibodies can be developed against almost any surface of a given protein, in spite of some of these surfaces being fairly polar. To take advantage of these properties, we have developed an aADARS potential. This potential shows that the atom types YC^{ζ} and FC^{ζ} from Tyr, Trp and Phe residues (Zhang *et al.*, 1997) have a high probability of being in the paratope and favorably contribute to the interaction energy, regardless of the type of the atoms of the epitope they interact with.

To test our newly developed potential, we have performed a docking test on the antibody–antigen complexes of the protein–protein docking benchmark (Hwang *et al.*, 2008). Our results demonstrate that this potential is generally quite successful in discriminating near-native structures of antibody–antigen complexes. In fact, the potential is able to discriminate the paratope of the antibody using only biophysical methods, i.e. adding *a priori* information on the location of the CDR regions did not improve the docking results. We believe that more data (i.e. more resolved crystal structures of antibody–antigen complexes) would improve the potential even further. As we noted, there were relatively few contacts for a number of the atom types. More structures would ameliorate this problem, possibly allowing for the introduction of additional atom types and thus enabling the development of more detailed antibody–antigen potentials. We note that the asymmetric properties of interfaces are not constrained to antibody–antigen complexes. In particular, many signal transduction complexes of the docking benchmark set exhibit similar features. This is a topic of our current research.

Another direction of research in docking antibodies which needs improvement is the ability to work with the models rather than experimental structures. Despite the fact that antibody models are usually extremely precise, the quality of docking results tends to drop drastically when using models rather than real structures. Accordingly, CAPRI targets that involve docking based on homology models (Lensink and Wodak, 2010) are not modeled well. The reason for this drop in performance can be explained by the fact that standards for modeling proteins and the quality of the structures needed for docking are very different. For example, we know that side-chains placement is extremely important for protein docking and it is totally ignored in assessment of quality for protein models. Also side-chain placement strongly depends on the backbone and slight deviation of the backbone, which will be unnoticeable in the protein model quality, will strongly affect side-chain distribution, and hence the docking results.

AVAILABILITY AND IMPLEMENTATION

We have added the antibody–antigen docking mode to our protein–protein docking server ClusPro (Comeau *et al.*, 2007). The server is hosted at 'http://cluspro.bu.edu.' ClusPro is freely available to the academic community. For convenience of job tracking, and privacy users can create an account, however it is not required. To access the server without login users should either click the link 'Use the server without benefits of your own account' or use the direct link 'http://cluspro.bu.edu/nousername.php.'

ACKNOWLEDGEMENTS

For the CPU time used for this article, the authors thank the Boston University Scientific Computing and Visualization Center for the opportunity of running the PIPER program on the Blue Gene/L supercomputer.

Funding: National Institute of General Medical Sciences [GM61867 to S.V. and GM93147 to D.K.], National Science Foundation [DBI 1147082 to S.V. and D.K.], and USA-Israel Binational Science Foundation [2009418 to O.F. and D.K].

Conflict of Interest: None declared.

REFERENCES

Chen,R. *et al.* (2003) ZDOCK: an initial-stage protein-docking algorithm. *Proteins*, **52**, 80–87.

Chuang,G. *et al.* (2008) DARS (Decoys as the Reference State) potentials for protein–protein docking. *Biophys. J.*, **95**, 4217–4227.

Clark,L.A. *et al.* (2006) Trends in antibody sequence changes during the somatic hypermutation process. *J. Immunol.*, **177**, 333–340.

Comeau,S.R. *et al.* (2004) ClusPro: an automated docking and discrimination method for the prediction of protein complexes. *Bioinformatics*, **20**, 45–50.

Comeau,S.R. *et al.* (2007) ClusPro: performance in CAPRI rounds 6-11 and the new server. *Proteins*, **69**, 781–785.

Glaser,F. *et al.* (2001) Residue frequencies and pairing preferences at protein–protein interfaces. *Proteins*, **43**, 89–102.

Gray,J.J. *et al.* (2003) Protein–protein docking with simultaneous optimization of rigid-body displacement and side-chain conformations. *J. Mol. Biol.*, **331**, 281–299.

Halperin,I. *et al.* (2002) Principles of docking: an overview of search algorithms and a guide to scoring functions. *Proteins*, **47**, 409–443.

Hwang,H. *et al.* (2008) Protein–protein docking benchmark version 3.0. *Proteins*, **73**, 705–709.

Kozakov,D. *et al.* (2005) Optimal clustering for detecting near-native conformations in protein docking. *Biophys. J.*, **89**, 867–875.

Kozakov,D. *et al.* (2006) PIPER: an FFT-based protein docking program with pairwise potentials. *Proteins*, **65**, 392–406.

Kozakov,D. *et al.* (2008) Discrimination of near-native structures in protein–protein docking by testing the stability of local minima. *Proteins*, **72**, 993–1004.

Kozakov,D. *et al.* (2010) Achieving reliability and high accuracy in automated protein docking: cluspro, piper, sdu, and stability analysis in capri rounds 13-19. *Proteins*, **78**, 3124–3130.

Lensink,M.F. and Wodak,S.J. (2010) Docking and scoring protein interactions: capri 2009. *Proteins*, **78**, 3073–3084.

Lo Conte,L. *et al.* (1999) The atomic structure of protein-protein recognition sites. *J. Mol. Biol.*, **285**, 2177–2198.

Lu,H. and Skolnick,J. (2001) A distance-dependent atomic knowledge-based potential for improved protein structure selection. *Proteins*, **44**, 223–232.

Miyazawa,S. and Jernigan,R. (1985) Estimation of effective interresidue contact energies from protein crystal structures: quasi-chemical approximation. *Macromolecules*, **18**, 534–552.

Ponomarenko,J.V. and Bourne,P.E. (2007) Antibody–protein interactions: benchmark datasets and prediction tools evaluation. *BMC Struct. Biol.*, **7**, 64.

Ravikant,D.V.S. and Elber,R. (2010) Pie-efficient filters and coarse grained potentials for unbound protein–protein docking. *Proteins*, **78**, 400–419.

Rojnuckarin,A. and Subramaniam,S. (1999) Knowledge-based interaction potentials for proteins. *Proteins*, **36**, 54–67.

Sippl,M.J. (1993) Boltzmann's principle, knowledge-based mean fields and protein folding. An approach to the computational determination of protein structures. *J. Comput. Aided Mol. Des.*, **7**, 473–501.

Sircar,A. and Gray,J.J. (2010) Snugdock: paratope structural optimization during antibody–antigen docking compensates for errors in antibody homology models. *PLoS Comput. Biol.*, **6**, e1000644.

Skolnick,J. *et al.* (1997) Derivation and testing of pair potentials for protein folding, when is the quasichemical approximation correct? *Protein Sci.*, **6**, 1–13.

Vajda,S. (2005) Classification of protein complexes based on docking difficulty. *Proteins*, **60**, 176–180.

Zhang,C. *et al.* (1997) Determination of atomic desolvation energies from the structures of crystallized proteins. *J. Mol. Biol.*, **267**, 707–726.